

# Mathematical Modeling Experimental Approach of the Friction on the Tool-Chip Interface of Multicoated Carbide Turning Inserts

Samy E. Oraby and Ayman M. Alaskari

**Abstract**—The importance of machining process in today's industry requires the establishment of more practical approaches to clearly represent the intimate and severe contact on the tool-chip-workpiece interfaces. Mathematical models are developed using the measured force signals to relate each of the tool-chip friction components on the rake face to the operating cutting parameters in rough turning operation using multilayers coated carbide inserts. Nonlinear modeling proved to have high capability to detect the nonlinear functional variability embedded in the experimental data. While feedrate is found to be the most influential parameter on the friction coefficient and its related force components, both cutting speed and depth of cut are found to have slight influence. Greater deformed chip thickness is found to lower the value of friction coefficient as the sliding length on the tool-chip interface is reduced.

**Keywords**— Mathematical modeling, Cutting forces, Friction forces, Friction coefficient and Chip ratio.

## I. INTRODUCTION

MACHINING processes stems its importance from being a major manufacturing method where some statistics [1] indicates that about 15% of all mechanical components manufactured worldwide are derived from machining operations. However, it still one of the least understood manufacturing operations due to low predictive ability of the many proposed machining models [1]. Productivity enhancement at lower power requirements usually represents the ultimate objective of a machining process. While productivity is achieved through the use of higher levels of operating cutting parameters (speed, feed and depth of cut), the consumed power in the process depends to great extents on the environment tribological conditions at the tool-chip-workpiece interfaces. A proper manipulation of the technical junction between productivity enhancement and power reduction is still required since, as stated by many investigators, for example [2], there is still lack of fundamental understanding of the phenomenon occurring at the tool-chip and the tool-workpiece interfaces.

Many approaches have emerged within the last century to deal with metal cutting and machining dilemma with little eventual technical and applied benefits. Common research attempts regarding metal cutting and machining may be generally categorized into: analytical modeling, semi-analytical method, simulation and numerical techniques, empirical mathematical modeling and, inprocess monitoring systems. All these techniques aimed at the optimizing the cutting process through

the proper selection of the cutting parameters using an ideally designed cutting tool.

Most modeling approaches were more or less based on the Merchant orthogonal cutting model [3], Fig. 1.a, through studying the formation of continuous chip by assuming that the chip is formed by shearing along a shear plane whose inclination is obtained from the minimum energy principle. Many subsequent models were proposed [4-8] to add more reality to the orthogonal model proposed by Merchant. Kilicaslan [9] claimed that analytical methods have limited applications due to complexity of cutting processes. Instead, he added, Finite Elements Analysis (FEA) simulation became main tool to predict cutting variables such as forces, stresses, temperature, chip shapes, etc. without carrying on any money and time consuming experiments. Surprisingly, it was further admitted by [9] that the use of a simplified orthogonal, rather than oblique model was a necessity in FEA due its simplicity and being give good approximations. On contrary, it is reported [10] that FEA could provide much more detailed information about process but could be a very time consuming.

The use of advanced coating on carbide tools not only allowed accelerating the cutting speed with prolonged tool life but also improving the friction and tribological features in the tool-chip-workpiece interfaces. The use of TiN coating reduces tool replacement cost and improves surface quality as a result of the wear resistance of the substrate and not the coating layer [11-15]. According to [12], while TiC and Al2O3 appear to provide the most chemically stable screening layer between chip and tool, TiN, as a top coating layer, appears to offer the lowest tool friction and thereby low cutting temperature. Higher friction of TiC is due to the tendency of carbon content to diffuse from the TiC coating into the thin layer of steel that transfers to the tool surface, thus strengthening it. No such strengthening mechanism is evident when TiN is the coating [16]. As explained by Kassman [17], a smearing mechanism existed where TiN material was continuously transferred from coated to uncoated locations on the cutting edge (atomistic wear process) that led to the reduction of wear rate.

## II. FRICTION ON TOOL-CHIP INTERFACE

Studying friction is necessary to optimize cutting process since, as indicated by Astakhov [18], indicated that only 40-70% of the energy consumed by the cutting system is usually

spent to separate chip from workpiece material while, due to unoptimized tribological processes, the rest (30-60%) ineffective energy is used merely in the transition of the useful energy into the tool-chip and tool-workpiece interfaces. A reduced cutting force is beneficial, primarily because it demands less motor power and ensures stability of the cutting machine [12]. Force system in metal cutting was first proposed by Merchant [3], Fig. 1.a. The total force is represented by two equal, opposite forces (action and reaction)  $R$  and  $R'$  which hold the chip in equilibrium, Fig.

1.b. The force,  $R'$ , which the tool exerts on the chip is resolved into the tool face-chip friction force ( $F$ ) and normal force ( $N$ ). The force,  $R$ , which the workpiece exerts on the chip, is resolved along the shear plane into the shearing force, ( $F_s$ ) which is responsible for the work expended in shearing the metal, and into normal force ( $F_n$ ), which exerts a compressive stress on the shear plane. Force  $R$  is also resolved along the direction of tool motion into ( $F_c$ ), termed by Merchant as the cutting force, and into  $F_t$ , the thrust force, Fig. 1.c.

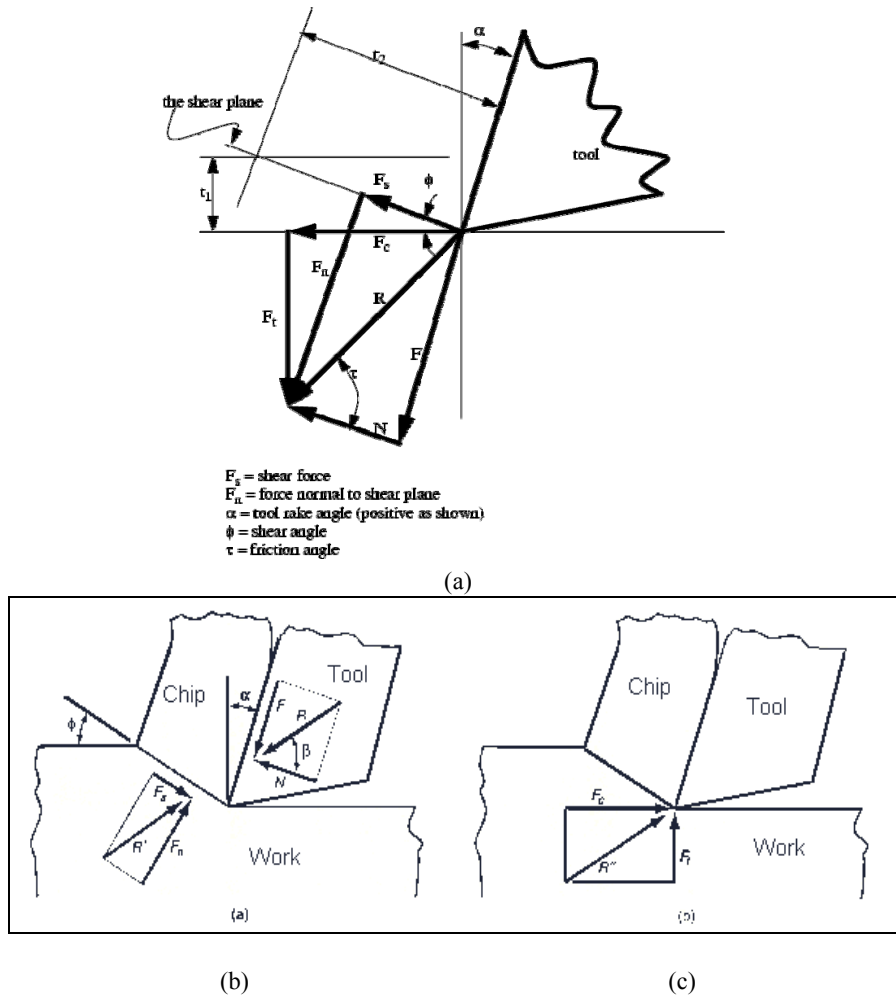


Fig.1 Merchant's force model General

According to Merchant force model, cutting ( $F_c$ ) and thrust ( $F_t$ ) force components can be transformed to normal ( $N$ ) and friction ( $F$ ) components apply on the tool face as follows:

$$F = F_c \sin(\alpha) + F_t \cos(\alpha) \quad (1)$$

$$N = F_c \cos(\alpha) - F_t \sin(\alpha) \quad (2)$$

in which ( $\alpha$ ) is the normal rake angle.

According to Coulomb law, the apparent coefficient of friction on tool-chip interface becomes:

$$\mu = \left[ \frac{F}{N} \right] = \left[ \frac{F_c \sin(\alpha) + F_t \cos(\alpha)}{F_c \cos(\alpha) - F_t \sin(\alpha)} \right] = \left[ \frac{\tau}{\sigma} \right] \quad (3)$$

where ( $\tau$ ) and ( $\sigma$ ) are the friction shear and normal stress on the tool-chip interface respectively. This implies that the Coulomb friction model can be used on the entire contact friction zone with a constant coefficient of friction ( $\mu$ ) or, that the frictional stress ( $\tau$ ) on the rake contact region is in a direct proportional to the normal stress ( $\sigma$ ) [19].

Astikhov [1] indicated that with the Coulomb model constant coefficient, any variation of temperature and pressure on the rake face was neglected. According to Kilicaslan [9], the Coulomb model is valid only when normal force ( $N$ ) was below a critical certain value where, in machining the friction conditions are very different from a simple dry friction where normal force is very high. As the normal force increases, Coulomb law no longer holds true as the real area of contact between chip and tool rake face increases [9]. Results by [5&20], Fig. 2, indicated that the shear friction stress ( $\tau$ ) remained constant over about the half of tool-chip contact nearest the cutting edge but it gradually decreased reaching zero when the chip departed contact with the rake face. The normal stress ( $\sigma$ ) was found to gradually decrease reaching zero at the chip departure point. Over the length AB, normal stress is sufficiently high and contact area approaches the total apparent area and metal adheres to the rake face. The coefficient of friction in this sticking region is not constant and is lower than the value under sliding friction conditions. In the length from B to C, which extends from the end of the sticking region to the point where chip loses contact with the tool rake face, the contact area to total area ratio is less than unity, so coefficient of friction is constant, and sliding friction occurs.

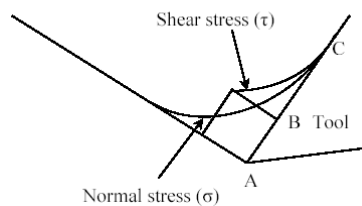


Fig. 2 Normal and friction stress distribution on the tool-chip interface

According to [9], the value of the coefficient of friction varies as relative values of both sticking and sliding lengths changes can be considered as the average value based on both sticking and sliding regions. According to [2], the apparent coefficient of friction is mainly determined by the adhesive phenomena since; around 90% of the apparent friction was due to adhesion while only 10% was due to plastic deformation. On contrast, Madhavan et al. [21] introduced a different view that sliding occurs over much of the interface near the cutting edge and sticking occurs near the boundary of tool-chip contact. A third different approach is proposed by Ackroyd et al. [22] where the tool-chip contact is composed of four distinct regions: a region of stagnation at the cutting edge, a region of retardation, a region of sliding followed by one of sticking near the boundary of the tool-chip contact. According to [10], while a maximum apparent friction coefficient value was 0.6 when carbide inserts were employed, a minimum friction coefficient value was measured to be around 0.3 for CBN with dry cutting conditions and uncoated

carbide insert with coolant. Due to the existence of the sticking region, they explained, the sliding coefficient of friction was found slightly greater than those for the apparent coefficient of friction. However, they indicated that when friction coefficient was high, thrust force, chip thickness, contact length, and shear angle were accurately predicted but inaccurate overestimated values of cutting forces and temperature were observed. Due to computational errors emerged with the analysis [9], the friction coefficients obtained from analytical relationships was not appropriate to be used in finite element simulation of metal cutting. The use of constant friction coefficient in most FEA analysis is criticized by Astakhov as this contradicts most of the available theoretical and experimental data. According to Dieter results [23], the most usual case is sticking friction, where there is no relative motion between the chip and the tool at their interface. A limiting value for coefficient of friction as 0.577 where, above this value, there is no relative motion can occur at the interface. This is criticized by Astakhov [1] explaining that this contradicted the facts evolved in the practice of metal cutting where in many experimental investigations, most values of friction coefficient are well above 0.577 and might reach 2.0. Results by [16] indicated that the measured coefficient of friction varied between 0.75 and 0.6 for the wide range of cutting speeds reported. As stated by [1], the values of coefficient of friction used in FEM modeling are always below the assumed limiting value just to suit the sliding condition at the interface.

Many different experimental techniques were used to measure the contact length on the rake face. Friedman and Lenz [24] determined the contact length by the microscopic examination of the traces left by the sliding chip on the rake face. Another technique was proposed by Iqbal et al [25] by using the underside tracks of the chip. According to FEA numerical study [9], the contact length was calculated as 0.35 mm and the sticking region length is calculated as 0.06 mm. However, in a study by Shatla et al. [26], the length of the sticking region was assumed to be two times of the uncut chip thickness. Ozel and Budak [10] disagreed with the above the overestimated value suggesting that the length of the sticking zone was equal to only the uncut chip thickness.

As concluded by [16], the tool chip contact length increases with increasing chip compression ratio explaining that, at a reduced chip compression ratios (thinner chips) promote chip curl and hence reduce contact length and hence the friction coefficient.

From the above seemingly discussion, there is still no consolidating evidence to introduce to those involved in practical metal cutting and machining. Unfortunately, from shopfloor applications viewpoint, none of these achieved a decisive and convincing victory. The problem resides in the way the two terminologies: "Machining" and "Metal Cutting" is long handled and practically interpreted. Although both terms are long considered identical, it is thought that they have a quite disparity technical interpretation. Machining generally defines alteration in workpiece configuration (visible

responses) before and after processing such as surface roughness, dimensional accuracy, system stability, etc. Metal cutting, on the other hand, is the term to deal with the principles of most relevant invisible process parameters such as shear stress, strain rate, friction, wear rate, etc. Although all metal cutting parameters are considered as controlling elements of the machining responses, the most practical interests are extensively directed toward the understanding of the machining aspects rather than to the metal cutting principles. Technical confusion may emerge, for instance in turning operations, when cutting speed is apparently assessed without the consideration of work diameter. A high revolution rate (RPM) may give a deceiving impression about the velocity (distance rate) when it is associated with smaller workpiece diameter. From a machinist viewpoint, high RPM has a significant influence on machine and workpiece stability but, for a metal cutting theory researcher, its effect is not assessed without knowing the workpiece diameter.

Analytical predictive modeling approach considering too many parameters doesn't necessary benefit the ultimate practical objectives. This is due the well known problem of cutting variability which may far exceeds any possible contribution offered by a complex analytical model [27]. In brief, all what a machining engineer or, a technician needs is some helpful machinability data to optimize the process through the selection of the appropriate cutting conditions. Moreover, most studies in metal cutting are concentrated on the improvement of cutting tool performance that adds little to productivity. According to latest enormous advancement in tool and workpiece technology, machining cost now depends to great extent on the optimal utilization of machine capacity to increase productivity. This may be the reason behind the wide acceptance ground of the inprocess approach where the process is continuously monitored online and, whenever needed, a manual or an automatic action is taken to retain a proper stable condition. Adaptive control (AC) of machine tools, in its two common sections; adaptive control optimization (ACO) and adaptive control constraints (ACC), has recently gained expandable ground. However, many control systems and instrumentation problems have to be solved before a commercially acceptable AC is feasible. Mathematical modeling and empirical approaches rather than complex analytical models can play an important role in AC implementation, for instance [28].

The current study is an empirical approach to evaluate the friction phenomenon on the tool-chip interface using the measured cutting forces components. Friction coefficient, friction force and normal friction force are related to the dependent operating parameters as well as the chip ratio.

### III. EXPERIMENTAL PROCEDURES AND SETUP

Experiments are carried out to conform reasonably to practical rough operations. To insure modeling statistical adequacy and significance, cutting parameters; cutting speed (V), feed rate (f) and depth of cut (d) are specified according to

central composite design CCD to constitute a total of 24-experiment in four blocks, Table I.

Two machining combinations were carried out in the study. The first combination was the use of multicoated carbide inserts (Sandvik 435) to cut 709M40 (EN19) high tensile stress chromium alloy steel while the second was the use of multicoated carbide inserts (Sandvik GC415) to cut 817M40 (EN24) alloy steel. Both insert types consist of three coating layers: 1  $\mu$ m TiN followed by 3  $\mu$ m Al<sub>2</sub>O<sub>3</sub> and finally a layer of 5  $\mu$ m TiC over the sintered carbide substrate. As recommended by manufacturer, GC435 inserts are most appropriate for steel cutting (ISO P35 range) with decreasing rates of plastic deformation and growth of thermal and mechanical fatigue cracks while GC415 inserts are intended for turning steel and cast iron (P05-30, K05-20, C6-8). Both insert types were of SPUN 12 03 12 configuration (thickness = 3.18 mm & r=1.2 mm & l=12.7 mm). Inserts were clamped to a Sandvik CSTPRT-MAX tool holder with seat configuration 6°, 5°, 0°, 60°, 90° normal rake, clearance, inclination, approach and side approach angles respectively.

Three cutting force components: main (F<sub>c</sub>), feeding (F<sub>f</sub>) and radial (F<sub>r</sub>), Fig. 3, were measured using a three-component dynamometer that replaced the tool post of a Colchester Mascot 1600 turning lathe. Force components are measured at the beginning of each test just few moments after signal stabilization and early enough before any wear or deformation mode(s) to develop. Samples of measured force signals are shown in Fig. 4.

### IV. MATHEMATICAL MODELING OF FRICTION ON THE RAKE FACE

The friction parameters at the rake face of three dimensions cutting, Fig. 3, can be considered as indicated by eqns. 1&3. Thrust force (F<sub>t</sub>) is determined as the resultant of the feeding (F<sub>f</sub>) and the radial (F<sub>r</sub>) components, Fig. 3 so that:

$$F_t = \sqrt{F_f^2 + F_r^2} \quad (4)$$

For (P) independent variables, any measured friction response (RF) can be represented by the general nonlinear multiplicative form is:

$$R_F = c \left[ \prod_{j=1}^p \xi_j^{\beta_j} \right] \varepsilon^{\wedge}, \quad (5)$$

in which  $\xi_j$  are the natural machining parameters (speed, feed and depth of cut), c and  $\beta_j$  are the model parameters to be estimated using the experimental data, and  $\varepsilon^{\wedge}$  is the multiplicative random error. This nonlinear regression model in its natural form:

$$R_F = a_0 V^{a_1} f^{a_2} d^{a_3}, \quad (6)$$

where a's are the model coefficients to be determined by the nonlinear regression procedures using the experimental data.

For sake of comparison with nonlinear regression model (6), a first order linear model is proposed with the parameters in their natural values to take the form:

$$R_F = b_0 + \sum_{j=1}^p b_j \xi_j + \varepsilon_n \quad (7)$$

where  $\varepsilon_n$  is the error absolute value using linear non-transformed model. In terms of cutting parameters, the model

takes the final first order linear regression model:

$$R_F = b_0 + b_1(V) + b_2(f) + b_3(d) \quad (8)$$

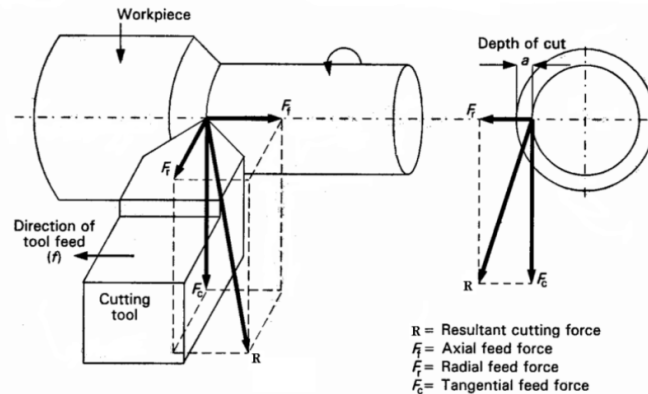


Fig. 3 Three dimensions cutting force system

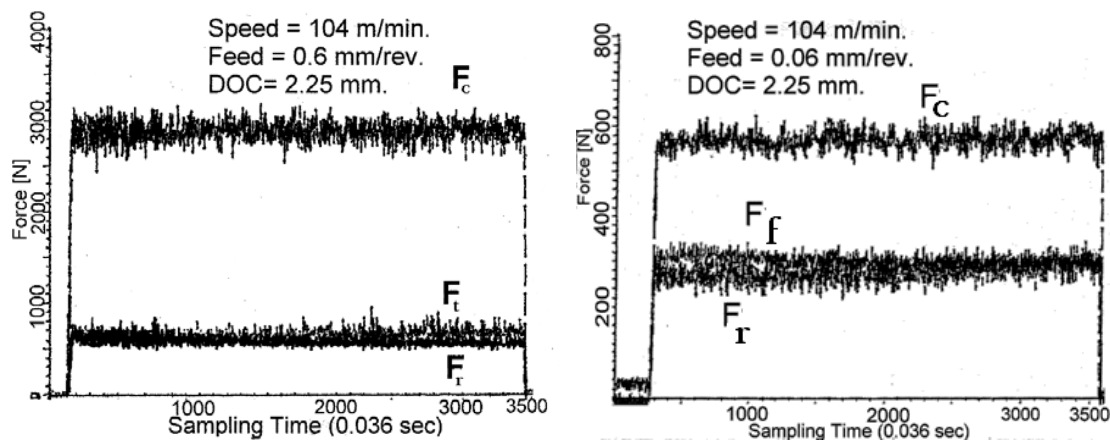


Fig. 4 Samples of the measured three force components

## V. RESULTS AND ANALYSIS

Coefficients for both nonlinear and linear proposed structures, eqns. 6&8 are individually determined for each of the measured  $F$ ,  $N$  and  $\mu$  friction components. Results of all possible linear and nonlinear estimation procedures are listed in Tables II.

Regression module, available in the SPSS commercial statistical computer software, is used throughout the estimation procedures. Various possible model structures are processed in order to evaluate the individual and the interaction influence of the operating independent parameters. The significance and adequacy of the estimated coefficients are assessed using the

associated statistical criteria, Table II.

### A. Coefficient of Friction

Regarding friction coefficient ( $\mu$ ), results in Table II indicate that the federate ( $f$ ) is the predominant influence with a negative effect. This is confirmed through the use of "Stepwise" routine in the linear regression procedures, model 2, Table II, where the feed was the only significant variable to include in the final model. In contrast to "ENTER" routine in the linear regression procedures where all variables are forced into the final model, "STEPWISE" is a selective procedure in such a way that only the statistically significant variable ( $s$ ) are included in the final model. The best general model to adequacy represent the whole set of the experimental data is

the nonlinear model 2, Table II:

$$\mu = 0.336 V^{(0.059)} f^{(-0.300)} d^{(-0.069)}, \quad R^2 = 92.9. \quad (9)$$

As indicated by Fig. 5, a noticeable decrease in  $\mu$  is observed as feed increases. A very slight positive effect of the cutting speed is detected by nonlinear modeling, Fig. 5.a. However, both linear and nonlinear techniques indicate a slight negative effect of the depth of cut, Fig. 5.b. According to Ozlu and Budak results [10], a slight decrease in friction coefficient with the cutting speed and the feed rate for each insert is observed. Between nonlinear and linear techniques, the former seems to have better statistical criteria represented by the model correlation factor  $R^2$  along with the coefficient individual standard error of estimates (SE) (compare nonlinear model no. 6 with the counterpart linear model no. 2, Table II).

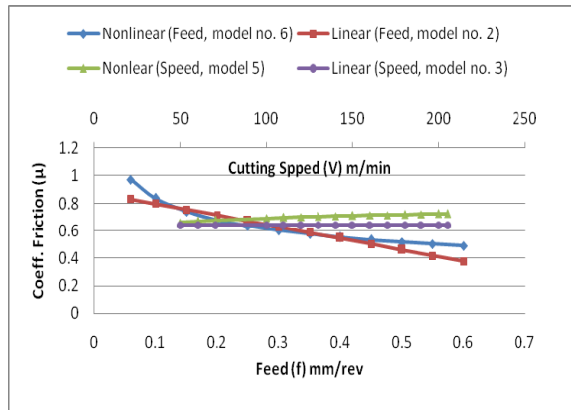
Surface representation and contour graphs of the relationship between coefficient of friction and both the cutting speed and feed is shown by Fig. 6. At lower feeds, friction coefficient is almost constant while it nonlinearly decreases as feed increases.

### B. Friction Force

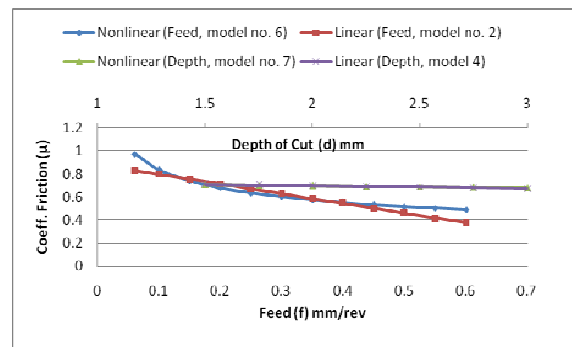
As shown by results listed in Table II, both nonlinear and linear modeling parameters for the friction force indicate a strong dependence basically on both the feed (higher  $R^2$ ) and the depth of cut (bigger coefficient value). This is logical since cutting force is usually affected by cut area. Within the employed range, cutting speed seems to have insignificant negative effect on the friction force. This agrees with the well established observations in a pioneer study by Arnold [29]. The best general model to adequately represent the experimental data is found to be the nonlinear model 1, Table II:

$$F = 852.4 V^{(-0.009)} f^{(0.424)} d^{(0.800)}, \quad R^2 = 95. \quad (10)$$

Three dimensional and contour graph of the effect of both feed and depth are shown in Fig. 7. On one hand, depth of cut produces almost twice as much impact on the friction force as feed does. Nonlinear superiority over linear is evident in both 3D and contour graphs where nonlinearity characteristics of the surface are well grasped.

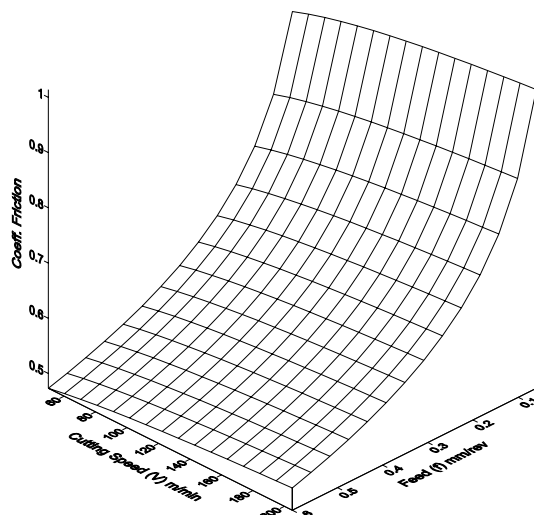


(a) Feed vs Cutting Speed



(b) Feed vs depth of cut

Fig. 5 Nonlinear and linear models of the effect of operating parameters on the coefficient of friction (GC435 coated inserts cuts 709M40 steel)



(a) Three dimensional graph

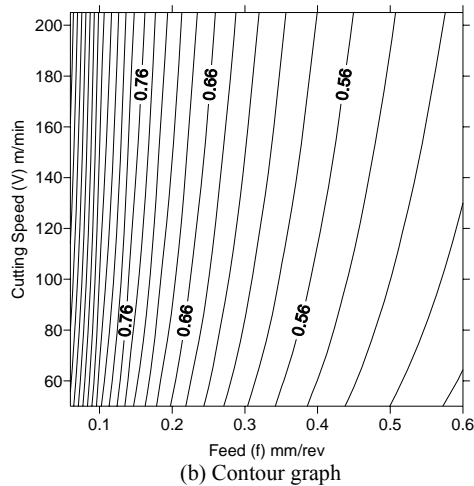


Fig. 6 Friction coefficient response surface as affected by feed and speed

### C. Normal Force

The final general nonlinear model to represent the experimental data for the normal force is found to take the form, Table II:

$$N = 2590.03 V^{(-0.049)} f^{(0.811)} d^{(0.896)}, \quad R^2 = 99.2 \quad (11)$$

As indicated in Table II, feed and depth of cut are found to be the main parameters affecting normal force (N) with almost equal impact. Feed, however, is found to have higher impact (bigger coefficient value of 0.81) and more statistical significance (better  $R^2$  of 91.5%) for normal than those for friction forces with counterpart values of 0.425 and 74% respectively. This may explain why the coefficient of friction ( $\mu$ ) is negatively affected by feed, eq. 9.

Depth of cut seems to have almost equal positive influence on both friction and normal forces and this explains why the

coefficient of friction ( $\mu$ ), as the ratio of the two components can be related only to feed without affecting the model adequacy. Figure 8 indicates the effect of cutting speed on F, N and  $\mu$ . Within the employed range, 50-200 m/min, coefficient of friction is found to increase from 0.665 to 0.725. However, a slight mixed effect is observed on both friction and normal forces [30].

As indicated by Fig. 9, further evidence exists that nonlinear modeling offers better and more accurate detection of the functional variability involved in the experimental results. Linear estimation tends to overestimate response value especially at four poles of the surface (operational domain).

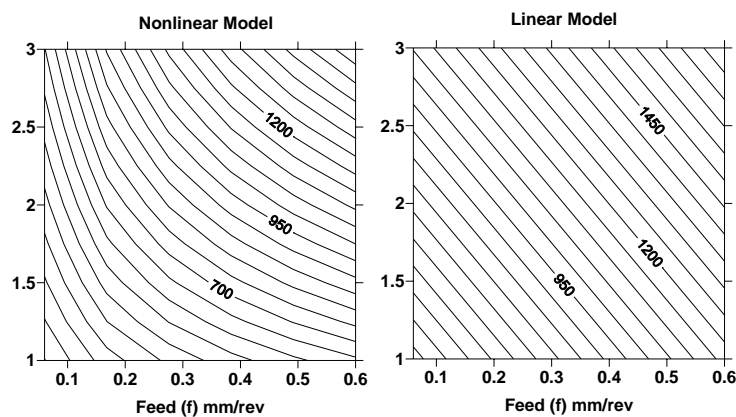
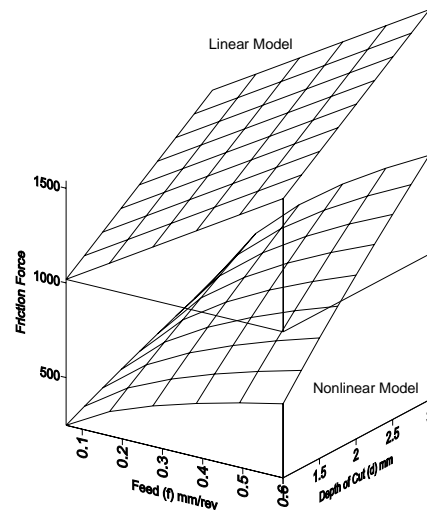


Fig. 7 Friction force linear and nonlinear response surface as affected by feed and depth

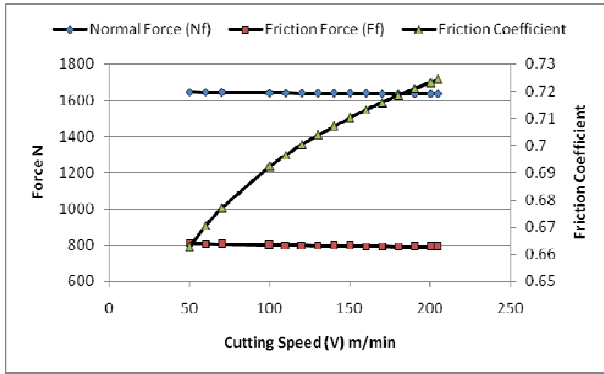


Fig. 8 Effect of cutting speed on the friction components

## VI. GENERAL EVALUATION AND DISCUSSIONS

### A. Modeling Credibility

To examine the credibility of the proposed empirical approach and its findings, it was necessary to repeat analysis considering an additional different cutting combination. Multilayers coated Sandvik GC415 is used to turn machine 817M40 (En24) high tensile alloy steel using the same setup as for GC435-709M40 combination. The resulting general significant nonlinear models are found to take the forms:

$$\mu = 0.207 V^{(0.19)} f^{(-0.261)} d^{(-0.037)}, \quad R^2 = 95. \quad (12)$$

$$F = 492.01 V^{(0.079)} f^{(0.340)} d^{(0.859)}, \quad R^2 = 92. \quad (13)$$

$$N = 2356.5 V^{(-0.108)} f^{(0.596)} d^{(0.877)}, \quad R^2 = 98. \quad (14)$$

The developed models indicate a similar trend to those for 709M40-GC435 for all friction components. Feedrate ( $f$ ) is found to have the predominant influence on the friction coefficient and its two components. The observation is confirmed not only by the feed high coefficient values but also by the associated enhanced statistical criteria of these coefficients. As feed increases, coefficient of friction tends to decrease gradually and nonlinearly. However, comparing to the first cutting set, feed usually is of lower impact on the friction force, eq. 13, while the case is reversed, eq. 14, when the normal force is considered. However, for GC415-817M40 cutting combination, cutting speed reveals higher consistent technological contribution with more enhanced statistical correlation factor. Nevertheless, speed coefficients indicate a positive effect on the friction force especially when cutting ratio is included into the final model. Correlation factor  $R^2$  is found relatively higher than those for the first cutting combination revealing a better dependence, or variability, within the experimental data of the second cutting combination. The influence of depth of cut on the friction parameters for GC415-817M40 shows almost similar behavior to that for GC435-709M40. However, the models constant coefficients (bo's) are of higher values for the latter. This is expected since this is directly proportional to specific cutting

energy of the machined workpiece and the functional variability extracted from the experimental data.

### B. Role of Chip Ratio ( $rc$ )

Since it is concluded that the feed is the most influential factor on the friction parameter, it is thought that the chip thickness on the rake face may play an important tribological role [9]. Therefore, chip ratio ( $rc$ ), deformed chip thickness / undeformed chip thickness, depends mainly on the cutting feed and the deformed chip thickness in the form:

$$\text{Chip\_Ratio}(rc) = \left[ \frac{t_c}{t} \right] = \left[ \frac{t_c}{f \sin(\kappa)} \right] = 1.1547 \left[ \frac{t_c}{f} \right] \quad (15)$$

where  $\kappa$  is the approach angle =  $60^\circ$ .

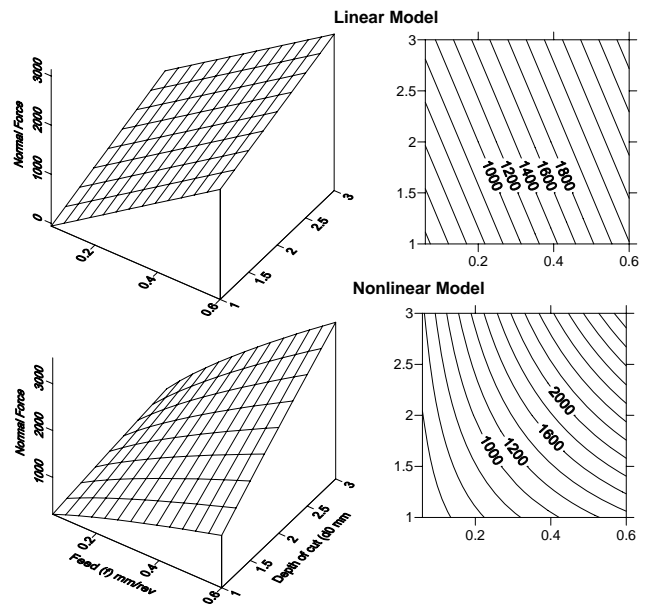


Fig. 9 Normal force linear and nonlinear surface as affected by feed and depth of cut

Nonlinear estimation procedures using the experimental data for GC415-817M40 combination has indicated a strong correlation between the friction components;  $F$ ,  $N$  and  $\mu$  and the chip thickness (chip ratio) along with cutting speed and depth of cut. This has led to the following best estimated models:

$$\begin{aligned} \mu &= 0.221(t_c)^{(-0.329)} V^{(0.179)}, & R^2 &= 95.5 \\ &= 0.115(r_c)^{(1.013)} V^{(0.271)}, & R^2 &= 86.8 \end{aligned} \quad (16)$$

$$\begin{aligned} F &= 391.38(t_c)^{(0.420)} V^{(0.117)} d^{(0.828)}, & R^2 &= 91.5 \\ &= 1266.77(r_c)^{(-1.452)} V^{(-0.06)} d^{(0.919)}, & R^2 &= 84.0 \end{aligned} \quad (17)$$

$$N = 1439.73 (t_c)^{(0.730)} V^{(-0.025)} d^{(0.823)}, \quad R^2 = 98.0$$

$$= 17976.7 (r_c)^{(-2.643)} V^{(-0.418)} d^{(0.999)}, \quad R^2 = 85.5 \quad (18)$$

Chip thickness ( $t_c$ ) shows positive impact that is twice as much on the normal than on the friction force, eqns. 17&18 thereby, it has a resultant negative effect on the coefficient of friction, eq. 16. This may be attributed to the relative change in sticking and sliding lengths on the rake face in such a way that thicker chip seems to increase sticking length permitting a smaller sliding action or, lower friction coefficient. This agrees with analysis by Iqbal et al [16] that sticking-sliding distribution schemes on the rake face do influence the chip curl and hence the contact length and chip back flow angle. However, they indicated that most contact length models are based on undeformed and deformed chip thickness, rake and shear angle while a great majority of the contact length models are independent of cutting speed.

## VII. CONCLUSION

Nonlinear regression as a mathematical modeling tool is found economical to well detect the functional nonlinearity and interaction features involved in the experimental data of the friction on the rake face. A strong correlation is found between the friction coefficient and the cutting federate in such a way that any increase in the employed feed lowers friction coefficient. Both cutting speed and depth of cut are found to have a slight effect on the friction coefficient. Within the whole set of experimental data, feed is found to carry about 74% of the inherent variability to represent the friction force modeling while only 21% is carried by the depth of cut. Regarding the normal force, those are found to be 91.5% and 7.5% for the feed and the depth respectively. Feed impact is found higher on the normal force than on the friction force while depth of cut indicates almost equal influence on both friction force components.

Deformed chip thickness is found to decrease the friction coefficient in such a way that thicker chip seems to increase sticking area (tool seizure effect) on the tool-chip. This may restrict sliding thereby lowers the friction coefficient.

As cutting goes on, it is expected that the process become more complex as wear scars are gradually developed on tool-face and flank. It is expected that this will lead to an entirely different friction mechanism as the coating-substrate topography is randomly damaged. This is currently intended in a further investigation by authors.

## REFERENCES

- [1] V.P. Astakhov, "On the inadequacy of the single-shear plane model of chip formation," *International Journal of Mechanical Sciences*, vol. 47, pp. 1649–1672, 2005.
- [2] F. Zemzemi et al., "Development of a friction model for the tool-chip-workpiece interfaces during dry machining of AISI4142 steel with TiN coated carbide cutting tools," *Int. J. Machining and Machinability of Materials*, vol. 2, no. 3, pp. 361–377, 2007.
- [3] E. Merchant, "Mechanics of the Metal Cutting Process I. Orthogonal Cutting and a Type 2 Chip," *Journal of Applied Physics*, vol. 16, no. 5, pp. 267–275, 1945.
- [4] J. D. Cumming, S. and E. G. Thomsen, "A New Analysis of the Forces in Orthogonal Metal Cutting," *ASME J. Eng. Ind.*, vol. 87, pp. 480–486, 1965.
- [5] N. N. Zorev, "Inter-relationship between shear processes occurring along tool face and shear plane in metal cutting," *International Research in Production Engineering, ASME, New York*, pp. 42–49, 1963.
- [6] E.H. Lee and B.W. Shaffer, "The Theory of plasticity applied to a problem of machining," *Trans. ASME, J. Appl. Mech.*, vol. 18, pp. 405–413, 1951.
- [7] M. C. Shaw, N.H. Cook, and I. Finnie, "The Shear-Angle Relationship in Metal Cutting," *Transaction ASME*, vol. 75, pp. 273–283, 1953.
- [8] W. B. Palmer and P. L. B. Oxley, "Mechanics of Orthogonal Machining," *Proc. Instn. Mech. Engrs.*, vol. 173, no. 24, pp. 623–638, 1959.
- [9] C. Kilicaslan, "Modelling and simulation of metal cutting by finite element method," *A M.Sc. thesis, Graduate School of Engineering and Sciences of Izmir Institute of Technology*, December 2009 IZMIR, Turkey.
- [10] E. Ozlu and E. Budak, "Experimental Analysis and Modeling of Orthogonal Cutting Using Material and Friction Models," in *4th International Conference and Exhibition on Design and Production of MACHINES and DIES/MOLDS, Cesme*, 2007, TURKEY, p. 23.
- [11] V.P. Astakhov, "Editorial: tribology at the forefront of study and research on metal cutting," *Int. J. Machining and Machinability of Materials*, vol. 2, no. 3, pp. 309–313, 2007.
- [12] B. Titus, B. Watmon and C. Anthony, "Coating Cutting Tools with Hard Substance Lowers Friction Coefficient and Improves Tool Life - A Review," in *Proceedings of the International MultiConference of Engineers and Computer Scientists 2010*, vol. III, IMECS 2010, Hong KONG, March 17–19, 2010.
- [13] S. Jacobson, S. Wallén P. Hogmark, S., "Intermittent metal cutting at small cutting depths Cutting forces," *International Journal of Machine Tools and Manufacture*, vol. 28, no. 4, pp. 551–567, 1988.
- [14] P. Wallén and S. Hogmark, "Influence of TiN coating on wear of high speed steel at elevated temperature," *Journal of Wear*, vol. 130, no. 1, pp. 123–135, 1989.
- [15] M. C. Shaw, "Metal cutting Principles," *Oxford University Press*, 2nd Ed, 2005.
- [16] S. A. Iqbal, P. T. Mativenga and M. A. Sheikh, "Contact length prediction: mathematical models and effect of friction schemes on FEM simulation for conventional to HSM of AISI 1045 steel," *Int. J. Machining and Machinability of Materials*, vol. 3, nos. 1/2, pp. 18–33, 2008.
- [17] P. Hedenqvist, M. Olsson, P. Wallén, A., Kassman, S. Hogmark and S. Jobson, "How TiN coatings improve the performance of high speed steel cutting tools," *Journal of Surface and Coatings Technology*, vol. 41, no. 2, pp. 243–256, 1990.
- [18] V. P. Astakhov, "Tribology of Metal Cutting," *London: Elsevier*, 2006.
- [19] Tugrul Ozel, "The influence of friction models on finite element simulations of machining," *International Journal of Machine Tools & Manufacture*, vol. 46, pp. 518–530, 2006.
- [20] E. Usui, and H. Takeyama, "A Photoelastic Analysis of Machining Stress," *Trans ASME, J. Eng. Industry*, pp. 303–308, 1960.
- [21] V. Madhavan, S. Chandrasekar and T. N. Farris, "Direct observation of the chip-tool interface in the low speed cutting of pure metals," *Transactions of the ASME, Journal of Tribology*, vol. 124, pp. 617–626, 2002.
- [22] B. Ackroyd, S. Chandrasekar and W. D. Compton, "A model for the contact conditions at the chip-tool interface in machining," *Transaction of ASME, Journal of Tribology*, vol. 125, pp. 649–660, 2003.
- [23] G. Dieter, "Mechanical metallurgy," *New York, McGraw-Hill*, 1976.
- [24] M. Y. Friedman and E. Lenz, "Investigation of the tool-chip contact length in metal cutting," *International Journal of Machine Tools Design*, vol. 10, pp. 401–416, 1970.
- [25] S. A. Iqbal, P. T. Mativenga and M. A. Sheikh, "Characterization of the Machining of AISI 1045 steel over a wide range of cutting speeds-Part 1: Investigation of contact phenomena," *Proceedings of IMechE Part B: Journal of Engineering Manufacture*, vol. 221, no. 5, pp. 909–916, 2007.
- [26] M. Shatla, C. Kerk and T. Altan, "Process Modelling in Machining. Part II: Validation and Applications of the Determined Flow Stress Data," *International Journal of Tools and Manufacturing*, vol. 41, pp. 1659–1680, 2001.

- [27] S. E. Oraby and A. M. Alaskari, "On the Variability of Tool Wear and Life at Disparate Operating Parameters," *Kuwait Journal of Science & Engineering (KJSE), An International Journal of Kuwait University*, vol. 35, no. 1B, 2008.
- [28] S.E. Oraby, E.A. Almeshaiei and A. ALASKARI, "Adaptive control simulation approach based on mathematical model optimization algorithm for rough turning," *Kuwait Journal of Science & Engineering (KJSE), An International Journal of Kuwait University*, vol. 30, no. 2, pp. 213-234, 2003.
- [29] R. N. Arnold, "The Mechanism of Tool Vibration in Cutting of Steel," *Proc. Inst. Mech. Engrs.*, vol. 27, pp. 261-276, 1946.
- [30] A. M. Bakkal, et al., "Chip formation, cutting forces, and tool wear in turning of Zr-based bulk metallic glass," *International Journal of Machine Tools & Manufacture*, vol. 44, pp. 915-925, 2004.

TABLE I  
CCD EXPERIMENTAL ARRANGEMENTS AND FORCE MEASUREMENT FOR GC435-709M40 COMBINATION

Seq	Cutting Conditions			Measured Forces [N]			Friction Parameters		
	Speed (V) m/min	Feed (f) mm/rev	DOC (d) mm	Cutting (F <sub>c</sub> )	Feeding (F <sub>f</sub> )	Radial (F <sub>r</sub> )	Friction Force (F)	Normal Force (N)	Friction Coeff. (μ)
T1	72	0.12	2.00	821	353	372	596	763	0.78102
T2	145	0.30	2.00	1490	483	487	838	1410	0.59419
T3	145	0.12	2.50	919	445	386	682	852	0.80001
T4	72	0.30	2.50	1853	621	545	1015	1756	0.57809
T5	104	0.20	2.25	1244	467	503	813	1165	0.69728
T6	104	0.20	2.25	1203	480	455	784	1127	0.69504
T7	145	0.12	2.00	745	396	330	591	687	0.85953
T8	72	0.30	2.00	1520	477	490	839	1440	0.58254
T9	72	0.12	2.50	1015	480	437	752	942	0.79830
T10	145	0.30	2.50	1862	618	563	1026	1764	0.58153
T11	104	0.20	2.25	1184	443	434	741	1113	0.66553
T12	104	0.20	2.25	1201	464	443	764	1127	0.67728
T13	206	0.20	2.25	1217	492	511	833	1136	0.73287
T14	50	0.20	2.25	1310	520	457	825	1230	0.67082
T15	104	0.60	2.25	2880	645	649	1211	2769	0.43742
T16	104	0.06	2.25	546	299	265	454	501	0.90657
T17	104	0.20	3.00	1472	532	503	882	1387	0.63572
T18	104	0.20	1.50	792	277	296	486	745	0.65205
T19	206	0.20	2.25	1217	512	549	874	1132	0.77000
T20	50	0.20	2.25	1306	547	507	878	1221	0.71936
T21	104	0.60	2.25	3055	686	750	1330	2932	0.45367
T22	104	0.06	2.25	551	319	288	485	503	0.96413
T23	104	0.20	3.00	1589	610	557	988	1494	0.66108
T24	104	0.20	1.50	793	301	333	529	742	0.71361

TABLE II  
NONLINEAR AND LINEAR ESTIMATION OF THE FRICTION PARAMETERS FOR GC435-709M40 COMBINATION

No.	<b>A) Nonlinear Model: <math>R = a_0 V^{a_1} f^{a_2} d^{a_3}</math></b>														
	Coefficient of Friction ( $\mu$ )					Friction Force (F)					Normal Friction Force (N)				
	Coefficients (SE)				Stat Crit.	Coefficients (SE)				Stat Crit.	Coefficients (SE)				Stat Crit.
	a0	a1	a2	a3	R <sup>2</sup>	a0	a1	a2	a3	R <sup>2</sup>	a0	a1	a2	a3	R <sup>2</sup>
1	0.336 (0.053)	0.059 (0.031)	-0.300 (0.019)	-0.069 (0.069)	92.6	852.4 (167.08)	-0.009 (0.038)	0.424 (0.024)	0.800 (0.093)	95	2590.03 (363.3)	-0.049 (0.028)	0.811 (0.016)	0.896 (0.068)	99.2
2	0.319 (0.047)	0.059 (0.031)	-0.300 (0.019)		92.3	817.68 (66.66)		0.424 (0.024)	0.800 (0.09)	94.9	2065.08 (125.190)		0.811 (0.017)	0.896 (0.071)	99.1
3	0.542 (0.295)	0.063 (0.109)		-0.058 (0.243)	1.8	464.39 (343.35)	-0.019 (0.147)		0.783 (0.352)	21.2	858.73 (1205.63)	-0.061 (0.219)		0.814 (0.672)	7.8
4	0.442 (0.030)		-0.301 (0.020)	-0.068 (0.073)	91.3	1615.53 (655.63)	-0.007 (0.087)	0.425 (0.054)		73.7	5346.65 (2222.7)	-0.048 (0.089)	0.812 (0.05)		91.6
5	0.518 (0.258)	0.063 (0.107)			1.5	866.4 (651.19)	-0.017 (0.162)			000	1605.09 (2177.61)	-0.061 (0.285)			0.2
6	0.419 (0.016)		-0.300 (0.020)		91	1563.44 (123.6)		0.425 (0.053)		73.7	4272.42 (270.89)		0.813 (0.049)		91.5
7	0.725 (0.141)			-0.057 (0.240)	0.3	425.37 (123.990)			0.783 (0.344)	21.2	646.75 (360.7)			0.813 (0.657)	7.5
<b>B) Linear Model: <math>R = b_0 + b_1(V) + b_2(f) + b_3(d)</math></b>															
	b0	b1	b2	b3	R2	b0	b1	b2	b3	R2	b0	b1	b2	b3	R2
1	0.897 (0.087)	000 (000)	-0.842 (0.088)	-0.024 (0.034)	82.4 (EN)	-180.62 (102.06)	0.185 (0.35)	1385.28 (104.25)	288.56 (40.2)	91.9 (EN)	-737.31 (86.91)	-0.444 (0.3)	4311.2 (88.78)	472.66 (34.25)	99.2
2	0.883 (0.023)		-0.846 (0.088)		80.6 (SW)	-160.04 (92.83)		1383.22 (102.38)	288.62 (39.5)	91.8 (SW)	-786.74 (82.81)		4316.1 (91.33)	472.51 (35.26)	99.1
3	0.642 (0.077)	000 0.001			2.2 (EN)	798.26 (135.63)	0.021 (1.165)			000 (EN)	1353.13 (371.67)	-0.964 (3.194)			0.4
4	0.747 (0.176)			-0.024 (0.077)	0.4 (EN)	489.36 (48.965)		1383.22 (188.19)		71.7 (EN)	276.41 (71.78)		4316.1 (275.8)		91.8
5						151.19 (273.52)			288.62 (120.2)	20.8 (EN)	184.38 (812.03)			472.5 (356.9)	7.4